

# Delayed feedback induced directed inertia particle transport in a washboard potential

D. Hennig and L. Schimansky-Geier

*Institut für Physik, Humboldt-Universität zu Berlin, Newtonstr. 15, 12489 Berlin, Germany*

P. Hänggi

*Institut für Physik, Universität Augsburg, Universitätsstr. 1, 86135 Augsburg, Germany*

(Dated: December 3, 2018)

We consider motion of an underdamped Brownian particle in a washboard potential that is subjected to an unbiased time-periodic external field. While in the limiting deterministic system in dependence of the strength and phase of the external field directed net motion can exist, for a finite temperature the net motion averages to zero. Strikingly, with the application of an additional time-delayed feedback term directed particle motion can be accomplished persisting up to fairly high levels of the thermal noise. In detail, there exist values of the feedback strength and delay time for which the feedback term performs oscillations that are phase locked to the time-periodic external field. This yields an effective biasing rocking force promoting periods of forward and backward motion of distinct duration, and thus directed motion. In terms of phase space dynamics we demonstrate that with applied feedback desymmetrization of coexisting attractors takes place leaving the ones supporting either positive or negative velocities as the only surviving ones. Moreover, we found parameter ranges for which in the presence of thermal noise the directed transport is enhanced compared to the noise-less case.

PACS numbers: 05.40.-a, 02.50.Ey, 05.60.-k, 05.65.+b, 87.15.-v

## I. INTRODUCTION

Transport phenomena play a fundamental role in many physical systems. In this context, the theme of a ratchet dynamics has attracted considerable interest over the past years. This is particularly due to the fact that the ratchet effect assists the creation of a directed flow of particles without the presence of any bias force in the system. The ratchet dynamics has been mainly applied to biological or mesoscopic systems where Brownian motion in a periodic *asymmetric* potential together with dissipation enters in some form the problem and the directed motion is generated from nonequilibrium noise, see the various overviews on molecular and Brownian motors in Refs. [1]-[5]. On the other hand for periodic systems with maintained spatial symmetry the accomplishment of directed net motion necessitates that the system is exerted to additional biasing (symmetry-reducing) impacts. Here we consider particle motion in a washboard potential which is often employed as a paradigm to model transport in one-dimensional periodic and *symmetric* structures [6],[7]-[13]. A symmetric (unbiased) external force is assumed to rock the potential. Our aim is to demonstrate that directed particle transport can be achieved with the application of a time-delayed feedback method in a wide temperature range. Although the delayed feedback method was originally proposed by Pyragas [14] to stabilize unstable states in deterministic systems meanwhile it has been facilitated in various other contexts [15] among them there is also the control of purely noise-induced oscillations [16],[17]. Recently in the context of controlling transport in Brownian motors a feedback strategy has been successfully utilized for two ratchet systems interacting through a unidirectional de-

lay coupling [18]. The effect of time-delayed feedback on the rectification of thermal motion of Brownian particles has been studied in overdamped ratchet systems [19]-[25]. A recent experimental implementation using such a feedback mechanism for a flashing ratchet has been realized with an optical line trap: it has been observed that the use of feedback increases the ratchet velocity up to an order of magnitude [26], in agreement with theory.

Stabilization of chaotic motion in deterministic inertia ratchet systems to increase the current efficiency was considered in Refs. [27],[28]. Furthermore, an asymmetric ratchet potential with included time-delayed feedback was treated in the context of an inertial Brownian motor [29].

Our paper, dealing with time-delayed feedback induced directed motion, is organized as follows: First we introduce the model of an inertial Brownian particle evolving in a symmetric spatially periodic potential under the influence of an additional time-delayed feedback term. The subsequent section concerns the underlying deterministic dynamics. In particular bifurcation diagrams with and without applied time-delayed feedback are discussed. The impact of a heat bath of fixed temperature on the particle transport features is studied in Section IV. Finally we summarize our results.

## II. THE MODEL

We consider an inertia Brownian particle that is moving along a one-dimensional periodic structure. The dynamics is governed by the following inertial Langevin

equation expressed in dimensionless form

$$\ddot{q} + \gamma \dot{q} = -\frac{dU}{dq} + F \sin(\omega t + \theta_0) + \xi(t) + f(t). \quad (1)$$

The dot denotes differentiation with respect to time. The particle evolves in a spatially-periodic and *symmetric* potential

$$U(q) = U(q + 1) = -\cos(2\pi q)/(2\pi), \quad (2)$$

of unit period  $L = 1$  and barrier height  $\Delta E = 1/\pi$  and its position and velocity are quantified by the variable  $q(t)$  and  $\dot{q}(t) \equiv v(t)$  respectively. The particle is driven by an external, time-dependent forcing field of amplitude  $F$ , frequency  $\omega$  and phase  $\theta_0$ . In addition it is subjected to a Gaussian distributed thermal, white noise  $\xi(t)$  of vanishing mean  $\langle \xi(t) \rangle = 0$ , obeying the well-known fluctuation-dissipation relation  $\langle \xi(t)\xi(t') \rangle = 2\gamma k_B T \delta(t - t')$  with  $k_B$  and  $T$  denoting the Boltzmann constant and temperature, respectively. The friction strength is measured by the parameter  $\gamma$ . The last term in Eq. (1) denotes a continuous time-delayed feedback term of the form

$$f(t) = K[\dot{q}(t - \tau) - \dot{q}(t)] \quad (3)$$

of strength  $K$  and with delay time  $\tau$ . Before we embark on the study of the Brownian particle motion it illustrative to consider the deterministic limiting case arising for vanishing thermal noise, i.e.  $T = 0$ . For our study we fix the following parameter values  $\gamma = 0.1$ ,  $\omega = 2.25$ ,  $\theta_0 = 0$ .

### III. THE DETERMINISTIC CASE

The dynamics of the deterministic system ( $T = 0$ ) exhibits very rich and complex behavior and depending on the parameter values and initial conditions one finds periodic, or aperiodic (quasiperiodic and/or chaotic) solutions in the long time limit [31]-[35]. The character of the phase flow evolving without feedback term ( $K = 0$ ) in a three-dimensional phase space is conveniently displayed by a Poincaré map using the period of the external force,  $T_e = 2\pi/\omega = 2\pi/2.25 \simeq 2.791$ , as the stroboscopic time. The deterministic equation of motion was integrated numerically and omitting a transient phase points were set in the map at times being multiples of the period duration  $T_e$ . In Fig. 1 (a) the bifurcation diagram as a function of the amplitude of the external driving is depicted.

Particle transport is quantitatively assessed by the mean velocity which we define as the time average of the ensemble averaged velocity, i.e.

$$v_m = \frac{1}{T_s} \int_0^{T_s} dt' \langle v_n(t') \rangle, \quad (4)$$

with simulation time  $T_s$  and with the ensemble average given by

$$\langle v_n(t) \rangle = \frac{1}{N} \sum_{n=1}^N v_n(t). \quad (5)$$

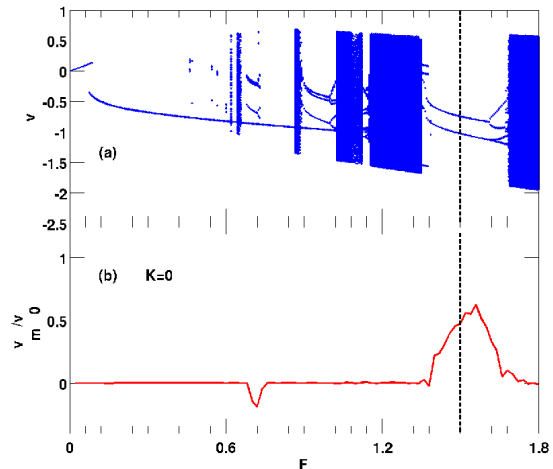


FIG. 1: (a): Bifurcation diagram as a function of the amplitude of the external driving without time-delayed feedback, i.e.  $K = 0$  and remaining parameter values:  $\omega = 2.25$ ,  $\gamma = 0.1$  and  $T = 0$ . (b): Mean velocity  $v_m/v_0$  as a function of the amplitude of the external driving. For later use a dashed vertical line is drawn at the value  $F = 1.5$

Here  $N$  denotes the number of particles constituting the ensemble with associated initial conditions  $q_n(0)$  and  $v_n(0)$  that are chosen such that the interior of the unperturbed separatrix in phase plane is uniformly covered. We express  $v_m$  in terms of the ratio of the spatial and temporal periods  $L/T_e \equiv v_0$  with  $v_0 \simeq 0.358$  being the velocity for running solutions that advance by one spatial period during one period duration of the external field.

For undercritical amplitudes of the modulation force  $F \lesssim 0.6$  those particles which are initially residing near the bottom of a potential well, remain trapped. Increasing  $F$  leads to escape from the potential wells and the particle jumps subsequently from one well to another one. The arising two typical scenarios are the pinned and running states respectively. In the former state the motion proceeds at most over a finite number of spatial periods whereas in the latter state motion is directed and unrestricted in the spatial dimension. In terms of the phase flow running asymptotic solutions correspond to phase locked periodic attractors transporting a particle with velocity  $v = m/n$  over  $m$  spatial periods of the potential during  $n$  period durations  $T_e$  of the external periodic field. Running asymptotic solutions may also be supported by aperiodic attractors.

In the bifurcation diagram associated with the dynamics without applied time-delayed feedback shown in Fig. 1 (a) one recognizes vertically extended stripes covered densely with points corresponding to non phase

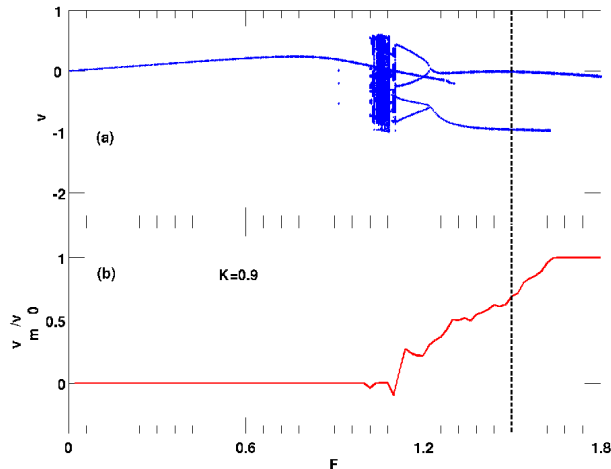


FIG. 2: As in Fig. 1 but with switched-on time-delayed feedback of strength  $K = 0.9$  and delay time  $\tau = 1.95$ . The remaining parameter values read as:  $\omega = 2.25$ ,  $\gamma = 0.1$  and  $T = 0$ .

locked aperiodic attractors and several periodic windows as well as period-doubling cascades to chaos. These features of the phase flow are readily attributed to the resulting mean velocity of the net motion (depicted in Fig. 1 (b)). The ensemble average is taken over an ensemble of  $N = 5000$  trajectories with uniformly distributed initial conditions  $q(0)$  and  $v(0)$ . For computation of the long-time average the simulation time interval for each trajectory is taken as  $T_s = 5 \times 10^5 \simeq 1.8 \times 10^5 \times T_e$ . We notice almost in the entire  $F$ -range vanishing mean velocity  $v_m = 0$ . The exceptions are the intervals  $0.74 \lesssim F \lesssim 0.80$  and  $1.36 \lesssim F \lesssim 1.62$  for which the solutions are associated with multiple coexisting attractors lying in fairly extended periodic windows in Fig. 1(a). Focusing interest on the latter one we note that at  $F \gtrsim 1.36$  tangent bifurcations give birth to two coexisting period-one attractors. The upper one of them is related with positive particle velocity  $v = v_0 > 0$  whereas on the lower one particles move with velocity  $v = -v_0 < 0$ . For increasing  $F \gtrsim 1.62$  these attractors are destroyed by way of crisis after passage through a period-doubling route to chaos.

The oppositely running solutions attributed to the two period-one attractors contribute to the mean velocity with different weight with the one with positive velocity  $v = v_0$  being *dominant* and thus yielding the window of positive mean velocity  $v_m$ . Apparently, the directed motion results from a lowering of the dynamical symmetry caused by the external modulation field [30],[13]. That is, even though the potential and the external modulation field are spatially and temporarily symmetric respec-

tively, with the choice of a fixed phase  $\theta_0$  the symmetry of the flow is reduced and a phase-dependent net motion is found. (Note that additional averaging over the phase  $\theta_0$  yields zero mean velocity.) Due to symmetry reasons it holds that the sign of the mean velocity is reversed upon the changes  $\theta_0 = 0 \rightarrow \theta_0 = \pi$  and  $F \rightarrow -F$  respectively. However, there exists a phase  $0 < \theta_0 < \pi$  for which symmetry between the two coexisting periodic attractors supporting solutions with velocities of opposite sign,  $v_0$  and  $-v_0$ , is restored and therefore the net motion vanishes.

In the numerical simulation of the system (1) with applied time-delayed feedback term (3) we set  $f(t) = 0$  in the interval  $t \in [0, \tau)$ , that is the system is affected by  $f(t)$  only for  $t \geq \tau$ . We performed extensive numerical studies to identify optimal parameters of the feedback term which establish efficient directed net motion. It turns out that this is achievable for delay times in the range of  $1.65 \lesssim \tau \lesssim 2.00$  and for feedback strength  $K \gtrsim 0.8$  (see also further below in Fig. 6). In the following we illustrate exemplarily the impact of time-delayed feedback on the transport properties for a feedback strength  $K = 0.9$  and delay time  $\tau = 1.95 \simeq 0.7 \times T_e$ . With such appropriate feedback term applied the extension of the aperiodic regions shrinks considerably and only a comparatively narrow band of aperiodic behavior for  $1 \lesssim F \lesssim 1.11$  prevails in the bifurcation diagram illustrated in Fig. 2 (a). Remarkably, for  $F \gtrsim 1.63$  the lower period-one attractor supporting negative velocities loses stability and is converted into a repeller leaving the upper attractor of positive velocity as the only persisting attractor. Thus application of feedback results in a reshaping of the bifurcation diagram. In fact, due to the absence of the period-one attractor supporting motion with velocity  $v = -v_0$  only running solutions with velocity  $v_m = v_0$  are then recognized in Fig. 2 (b) showing the mean velocity as a function of  $F$ . Otherwise the mean velocity raises from zero level for overcritical  $F \gtrsim 1.1$  and grows with increasing  $F$  until  $F \gtrsim 1.63$  when  $v = v_0$  is attained.

In order to gain insight into the feedback-induced mechanism that leads to directed transport (occurring for  $F \gtrsim 1.63$  in the period-one window in Fig. 2) we display the temporal behavior of the feedback term  $f(t)$ , given in Eq. (3), and the external driving term  $F(t) = F \sin(\omega t)$  and their sum  $F(t) + f(t)$  in Fig. 3 for driving amplitude  $F = 1.8$ . Throughout the time the feedback term  $f(t)$  performs oscillations possessing considerable asymmetry. Most importantly, these oscillations are entrained to the (symmetric) external driving term with a phase shift. The sum  $F(t) + f(t)$ , performing asymmetric oscillations, determines the *effective rocking force* exerted on the particle. This ratcheting force is self-induced due to the feedback in comparison with the externally imposed ratcheting force in the form of asymmetric periodic driving fields considered in [30].

How the directed rightward particle motion is enforced by this effective biasing rocking force is illustrated in

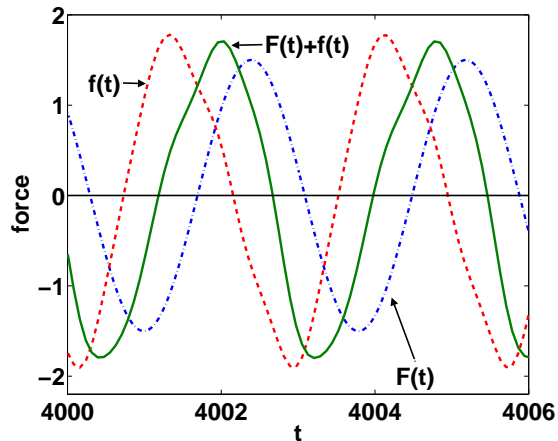


FIG. 3: Time evolution of the feedback term  $f(t)$ , the driving force term  $F(t)$  and their sum  $F(t) + f(t)$  with  $K = 0.9$  and delay time  $\tau = 1.95$ . The remaining parameter values read as:  $F = 1.8$ ,  $\omega = 2.25$ ,  $\gamma = 0.1$  and  $T = 0$ .

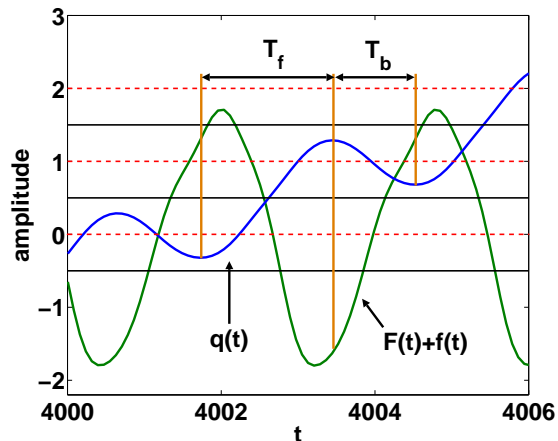


FIG. 4: Time evolution of the particle amplitude  $q(t)$  and the effective rocking force  $F(t) + f(t)$  with  $K = 0.9$  and delay time  $\tau = 1.95$ . The remaining parameter values read as:  $F = 1.8$ ,  $\omega = 2.25$ ,  $\gamma = 0.1$  and  $T = 0$ . Horizontal solid (dashed) lines indicate the position of the maxima (minima) of the unbiased washboard potential.

Fig. 4. (For the present discussion we discard the contribution from  $-dU(q)/dq$  to the total force.) Clearly, an oscillating rocking force leads to passages of forward and backward motion, also called enhancement and depreciation periods. Crucially, the feedback term is suitably entrained to the external driving term in such a way that the period of forward motion is longer than its backward counterpart, denoted by  $T_f$  and  $T_b$  respectively in Fig. 4. To be precise, at the moment when the backward motion of the particle terminates the effective rocking force has not yet reached its maximum as indicated by the left vertical line in Fig. 4. Subsequently the particle moves in the forward direction due to the ongoing positive rock-

ing force that after passing through its maximal value declines. Nevertheless, until half of the time span  $T_f$  is reached the particle motion is still enhanced in the forward direction. Afterwards for  $t > T_f/2$  the effective rocking force becomes negative and thus the momentum of the particle is reduced steadily with increasingly negative values of  $F(t) + f(t)$ . The end of the forward-motion period is designated by the middle vertical line in Fig. 4. However, there remains only comparatively little time, namely  $T_b < T_f$ , during which backward-motion is enforced, that is when during the depreciation period the effective rocking force is negative.

Consequently, the asymmetry in the enhancement and depreciation phases serves for a rather long period of forward-motion compared to the backward-motion. Therefore the effective motion of the particle proceeds to the right. Notably, this feature is induced by entrainment of the asymmetric time-delayed feedback term to the symmetric external modulation field if the feedback strength and delay time are suitably chosen. Notice that this oscillation behavior of the time-delayed feedback term is different from noninvasive control methods where the delayed feedback control vanishes once a targeted unstable periodic orbit has been stabilized [14],[15],[28],[29].

#### IV. DIRECTED THERMAL NET PARTICLE MOTION

We now study the impact of a heat bath of fixed temperature  $T > 0$  on the particle transport features. With the inclusion of finite thermal noise transitions between the now metastable attractors are likely and, independent of the initial conditions, trajectories permeate the whole phase space rendering the dynamics ergodic.

For the computation of the mean velocity the ensemble average in (5) was taken over  $N = 5000$  realizations of the thermal noise for an arbitrarily chosen initial condition. The mean velocity  $v_m$  represented without feedback term but in the presence of thermal noise of a fairly high level of  $k_B T = 0.1 \times \Delta E$  in Fig. 5(a) is zero regardless of the value of the modulation field strength  $F$ . This has to be distinguished from the preceding noise-less case where there exist even for  $K = 0$  regions of nonvanishing net motion (cf. Fig. 1) due to the fact that motion on attractors with different sign of the velocity contribute with distinct weight to the asymptotic net motion. In other words, the impact of the noise leads to symmetrization of the basins of attraction of transporting periodic and/or aperiodic attractors. Therefore any initial condition yields zero asymptotic current.

Interestingly, this situation changes imposing the Langevin dynamics additionally to the time-delayed feedback and we found parameter constellations for which directed net motion results despite the presence of strong noise.

As Fig. 5(a) reveals, applying feedback of strength  $K = 0.9$  and delay time  $\tau = 1.95$ , the mean velocity

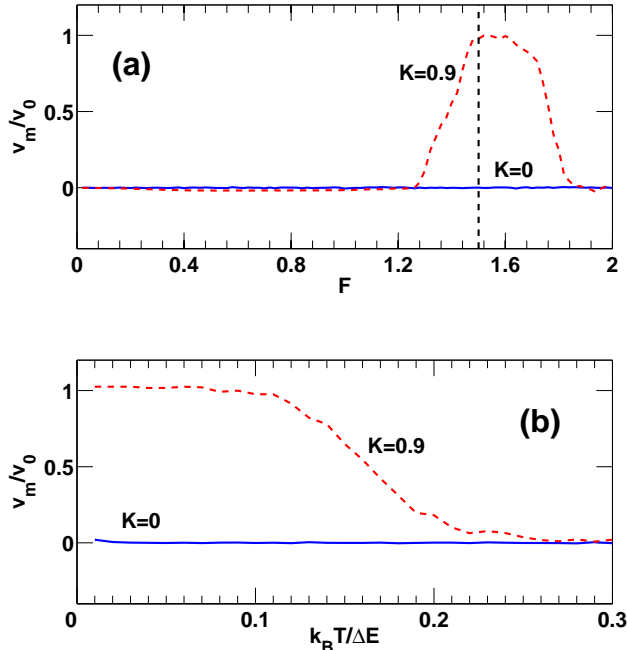


FIG. 5: (a): Mean velocity in dependence of the external modulation field amplitude without and with applied time-delayed feedback force as indicated in the plot and for thermal energy  $k_B T = 0.1 \times \Delta E$ . (b): Mean velocity in dependence of the thermal energy expressed in units of the barrier energy,  $k_B T / \Delta E$ , and for fixed  $F = 1.5$  and delay time  $\tau = 1.95$ . The remaining parameter values are  $\omega = 2.25$  and  $\gamma = 0.1$ .

as a function of the external modulation field strengths exhibits a resonance-like structure for  $1.2 \lesssim F \lesssim 1.7$ , i.e. for values of  $F$  for which transport exists in the deterministic case. Strikingly, with the impact of thermal noise the feedback-controlled transport proceeds more efficient in comparison with the deterministic case in the fairly wide range  $1.2 \lesssim F \lesssim 1.7$  (cf. Figs. 2 and 5 (a)). On the other hand, for  $F \gtrsim 1.7$  the directed transport feature of the deterministic system is destroyed by the thermal fluctuations. Furthermore, like in the deterministic case, there exist a threshold value for the feedback strength beyond which directed net motion is achieved (see Fig. 6 (a)) and the range of delay times being optimal for running solutions is indicated by the resonance-like structure in Fig. 6 (b).

From Fig. 5 (b), illustrating the mean velocity in dependence of the noise strength, one infers that directed transport is sustained up to comparatively high noise strength before it ceases eventually to exist. On the other hand, it is seen that without feedback term, i.e.  $K = 0$ , the mean velocity averages to zero already for low noise intensity. As the damping strength is concerned we found that feedback-induced directed motion is maintained as long as the system remains in the underdamped regime,

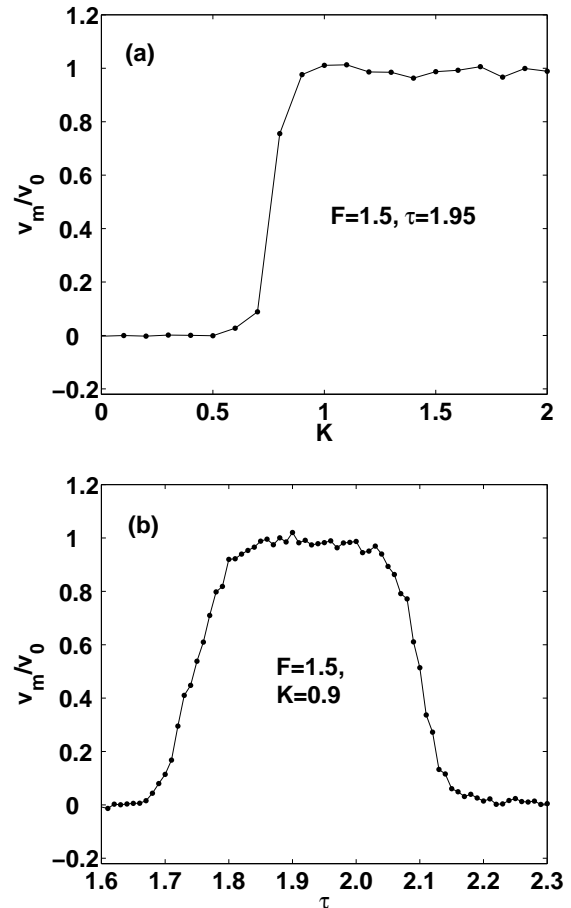


FIG. 6: (a) Mean velocity in dependence of the strength of the time-delayed feedback and for fixed  $F = 1.5$  and  $\tau = 1.95$ . (b): Mean velocity in dependence of the delay time and for fixed  $F = 1.5$  and  $K = 0.9$ . The remaining parameter values are  $\omega = 2.25$ ,  $\gamma = 0.1$  and  $k_B T = 0.1 \times \Delta E$ .

that is for  $\gamma \lesssim 2.5 \simeq \omega_0$  with  $\omega_0 = \sqrt{2\pi}$  being the frequency of harmonic oscillations near the bottom of a potential well.

Further insight into the origin of running solutions in the noise case is gained from Fig. 7 showing the stroboscopic map of the average trajectory defined as  $q_a = \sum_{n=1}^N q_n / N$  and  $v_a = \sum_{n=1}^N v_n / N$  with and without presence of the time-delayed feedback for external modulation strength  $F = 1.5$ , a value for which in the deterministic case the mean velocity remains nearly unaffected when the feedback is applied (to ease the eyes the vertical dashed line is drawn at the position of the value  $F = 1.5$  in Figs. 1, 2 and 5 (a)). Without feedback,  $K = 0$ , the velocity range of the average trajectory is not only symmetric with respect to  $v_a = 0$  but remains confined within the boundaries of the separatrix loop of the undriven, undamped deterministic system ( $\gamma = F = 0$ ). Thus the solutions represent pinned states. With applied feedback of strength  $K = 0.9$  the  $v$ -symmetry is broken. Moreover, the stroboscopic plot of the average trajectory

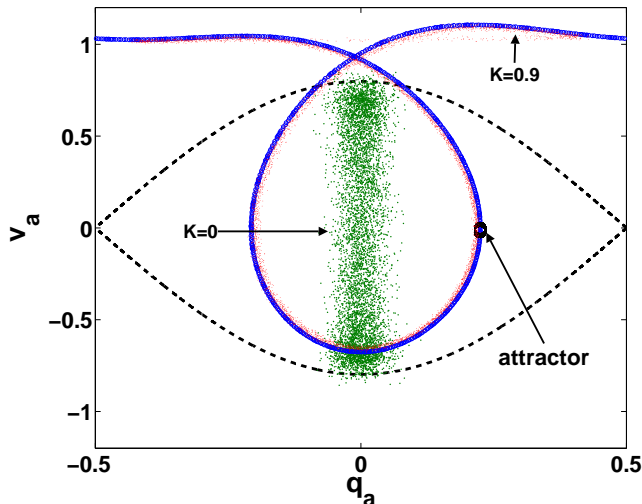


FIG. 7: Stroboscopic map of the average trajectory without ( $K = 0$ ) and with applied feedback ( $K = 0.9$  and  $\tau = 1.95$ ) as indicated in the plot. The remaining parameter values read as  $F = 1.5$ ,  $\tau = 1.95$  and  $k_B T = 0.1 \times \Delta E$ . The attractor with  $v = v_0 > 0$  of the deterministic system arising with the applied feedback is also shown. The dashed lines indicate the separatrix of the deterministic conservative undriven system, i.e.  $\gamma = F = 0$ . We also superimposed the projection of the orbit of the deterministic system on the  $v - q$ -plane (blue line).

densely covers the curve obtained when the periodic oscillations of the noise-less system are projected onto the  $q - v$ -plane. This implies the existence of an *attractive curve* related to near-torus-motion in phase space for the noise case. The corresponding stroboscopic map of the dominant deterministic periodic attractor with velocity  $v = v_0$  is also drawn in Fig. 7. Crucially for directed net motion with  $v_m = v_0$  arising for  $T > 0$  the average trajectory sticks to the near-torus motion never exploring other parts of the phase space during the whole simulation time interval  $T_s = 10^5$ . The time evolution of the corresponding average coordinate  $q_a$  is depicted in Fig. 8. Conclusively, despite the fact that the resulting motion in the presence of noise and feedback evolves no longer perfectly synchronous but still phase locked with the external periodic modulation it nevertheless exhibits behavior reminiscent of that found in the corresponding limiting deterministic system. To be precise the periodic oscillations of the deterministic dynamics are replaced by near-torus motion in the Langevin dynamics accomplishing phase locked aperiodic transport in the sense that on average during one period duration of the external field particles move by one spatial period, i.e.  $v_m = v_0 = L/T_e$ .

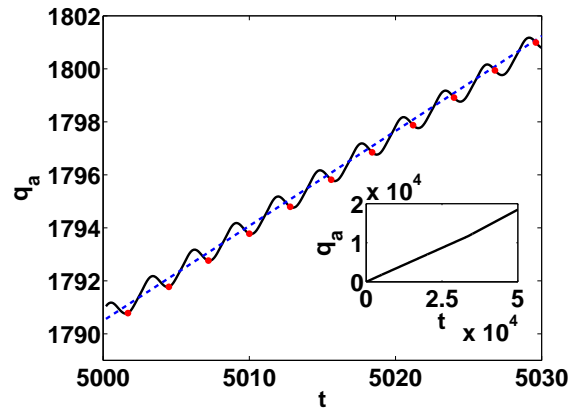


FIG. 8: Time evolution of the average coordinate  $q_a$  (wiggled line). The dashed straight possesses slope  $v_0 = L/T_e \simeq 0.358$ . The bullets represent the position of the particle at moments being multiples of the period duration of the external modulation  $T_e = 2\pi/\omega$ . The inset displays the long-time evolution of  $q_a$ . The parameter values read as  $F = 1.5$ ,  $K = 0.9$ ,  $\tau = 1.95$  and  $k_B T = 0.1 \times \Delta E$ .

## V. SUMMARY

In conclusion, we have identified and characterized a transport regime for underdamped Brownian particles evolving in a *symmetric* washboard potential under the mutual impact of an unbiased external periodic field and time-delayed feedback. We have studied first the deterministic case of zero temperature. It is has been shown that without feedback in some ranges of the amplitude and certain phases of the external modulation field windows of directed particle current exist. This is due to the fact that attractors associated with phase locked oppositely-running solutions contribute with different weight to the net current. The direction of the net current can be reversed with a suitable choice of the phase of the external modulation field.

Interestingly with an applied time-delayed feedback in the deterministic system there exist parameter ranges for which the attractors supporting velocities of a definite sign loose stability and are converted into repellers leaving the attractors of opposite velocity as the only persisting ones. Hence, the efficiency of the net particle current is improved. There exist values of the feedback strength and delay time for which the feedback term performs oscillations that are phase locked to the time-periodic external field. This yields an effective biasing rocking force, promoting periods of forward and backward motion of distinct duration, and thus directed motion.

On the other hand, for a finite temperature and without time-delayed feedback the net motion averages to zero. That is, the symmetry between the coexisting attractors supporting negative and positive velocities is restored by the impacting thermal fluctuations. Strikingly, in contrast to the case without feedback, with applied time-delayed feedback of appropriately chosen strength

and delay time we find in a wide temperature range complete desymmetrization of coexisting attractors supporting oppositely running solutions. As a consequence the particle motion proceeds exclusively in one direction. Therefore the feedback-induced transport is not only robust with respect to thermal noise but moreover, there exist parameter ranges for which in the presence of thermal noise the transport is more efficient than in the corresponding deterministic limiting case. We have identified attracting curves in phase space which are linked with motion on a torus with small deviations supporting transport.

We stress the difference between the transport control

mechanism described above and the control of transport properties in inertia ratchet systems [27],[28],[29] facilitating the stabilization of certain targeted (unstable) periodic orbits via time-delayed feedback as well as the features in feedback flashing ratchets when the potential is alternatively switched on and off in dependence of the state of the system [19]-[24]. In our case control of transport is achieved if the time-delayed feedback term with appropriately chosen strength and delay time entrains to the external time-periodic field yielding effectively a biasing force that rocks the washboard potential such that distinct durations of the periods of forward and backward motion ensue.

- 
- [1] P. Hänggi and R. Bartussek, *Lect. Notes Physics* **476**, 294 (1996).
- [2] F. Jülicher, A. Ajdari, and J. Prost, *Rev. Mod. Phys.* **69**, 1269 (1997).
- [3] R.D. Astumian and P. Hänggi, *Phys. Today* **55** (11), 33 (2002).
- [4] P. Hänggi, F. Marchesoni, and F. Nori, *Ann. Physik (Leipzig)* **14**, 51 (2005).
- [5] P. Hänggi, F. Marchesoni, *Rev. Mod. Phys.* **81**, 1 (2009).
- [6] H. Risken, *The Fokker-Planck Equation* (Springer-Verlag, New York, 1989).
- [7] F. Marchesoni, *Phys. Lett. A* **231**, 61 (1997).
- [8] G. Costantini and F. Marchesoni, *Europhys. Lett.* **48**, 491 (1999).
- [9] P. Reimann *et al* *Phys. Rev. Lett.* **87**, 010602 (2001)
- [10] D. Reguera *et al*, *Eur. Phys. Lett.* **57**, 644 (2002).
- [11] S.A. Tatarkova, W. Sibbett, and K. Dholakia, *Phys. Rev. Lett.* **91**, 038101 (2003).
- [12] E. Heinsalu, R. Tammelo, and T. Örg, *Phys. Rev. E* **69**, 021111 (2004).
- [13] D. Hennig, L. Schimansky-Geier, and P. Hänggi, *Eur. Phys. J. B* **62** 493 (2008).
- [14] K. Pyragas, *Phys. Lett. A* **170**, 421 (1994).
- [15] *Handbook of Chaos Control*, eds. E. Schöll and H.G. Schuster, 2nd ed. (Wiley-VCH, Weinheim, 2007).
- [16] N.B. Janson, A.G. Balanov, and E. Schöll, *Phys. Rev. Lett.* **93**, 010601 (2004).
- [17] T. Prager, H.P. Lerch, L. Schimansky-Geier, and E. Schöll, *J. Phys. A* **40**, 1 (2007).
- [18] M. Kostur, P. Hänggi, P. Talkner, and J. Mateos, *Phys. Rev. E* **72**, 036210 (2005).
- [19] F.J. Cao, L. Dinis, and J.M.R. Parrondo, *Phys. Rev. Lett.* **93**, 040603 (2004).
- [22] M. Feito and F.J. Cao, *Phys. Rev. E* **76**, 061113 (2007).
- [23] E.M. Craig *et al* *Europhys. Lett.* **81**, 10002 (2008); E.M. Craig *et al.*, *Ann. Phys.* **17**, 115 (2008).
- [22] M. Feito and F.J. Cao, *Phys. Rev. E* **76**, 061113 (2007).
- [23] E.M. Craig *et al* *Europhys. Lett.* **81**, 10002 (2008).
- [24] M. Feito and F.J. Cao, *Physica A* **387**, 4553 (2008).
- [25] D. Wu, S. Zhu, and X. Luo, *Phys. Lett. A* **372**, 2002 (2008).
- [26] B.J. Lopez *et al.*, *Phys. Rev. Lett.* **101**, 220601 (2008).
- [27] F. Family, H.A. Larrondo, D.G. Zarlunga, and C.M. Arizmendi, *J. Phys.: Condens. Matter* **17**, S3719 (2005).
- [28] W.-S. Son, Y.-J. Park, J.-W. Ryu, D.-U. Hwang, and C.-M. Kim, *J. Korean Phys. Soc.* **50**, 243 (2007); *Phys. Rev. E* **77**, 066213 (2008).
- [29] D. Wu and S. Zhu, *Phys. Rev. E* **73** 051107 (2006).
- [30] O. Yevtushenko, S. Flach, and K. Richter, *Phys. Rev. E* **61**, 7215 (2000); S. Denisov, S. Flach. A.A. Ovchinnikov, O. Yevtushenko, and Y. Zolotaryuk, *Phys. Rev E* **66**, 041104 (2002).
- [31] G.L. Baker and J.P. Gollub, *Chaotic Dynamics, an Introduction*, (Cambridge University Press, 1990).
- [32] R.L. Kautz, *Rep. Prog. Phys.* **59**, 935 (1996).
- [33] P. Jung, J.G. Kissner, and P. Hänggi, *Phys. Rev. Lett.* **76**, 3436 (1996).
- [34] D. Speer, R. Eichhorn, and P. Reimann, *Europhys. Lett.* **79**, 10005 (2007); *Phys. Rev. E* **76**, 051110 (2007).
- [35] M. Kostur, L. Machura, P. Talkner, P. Hänggi, and P. Talkner, *Phys. Rev. B* **77** (2008).
- [36] L. Machura, M. Kostur, P. Talkner, J. Luczka, and P. Hänggi, *Phys. Rev. Lett.* **98**, 040601 (2007).